JACS
JOURNAL OF THE AMERICAN CHEMICAL SOCIETY
Communication
pubs.acs.org/JACS

Ultrafast Interfacial Electron and Hole Transfer from $CsPbBr_3$ Perovskite Quantum Dots

Kaifeng Wu,[†,#] Guijie Liang,[†,‡,#] Qiongyi Shang,[†] Yueping Ren,[†,§] Degui Kong,[†,⊥] and Tianquan Lian*[,†]

[†]Department of Chemistry, Emory University, Atlanta, Georgia 30322, United States

[‡]Hubei Key Laboratory of Low Dimensional Optoelectronic Materials and Devices, Hubei University of Arts and Science, Xiangyang, Hubei 441053, China

[§]School of Environmental and Civil Engineering, Jiangnan University, Wuxi, Jiangsu 214122, China

[⊥]College of Electronic Engineering, Heilongjiang University, Harbin, HeilongJiang 150080, China

Supporting Information

ABSTRACT: Recently reported colloidal lead halide perovskite quantum dots (QDs) with tunable photoluminescence (PL) wavelengths covering the whole visible spectrum and exceptionally high PL quantum yields (QYs, 50−90%) constitute a new family of functional materials with potential applications in light-harvesting and -emitting devices. By transient absorption spectroscopy, we show that the high PL QYs (~79%) can be attributed to negligible electron or hole trapping pathways in $CsPbBr_3$ QDs: ~94% of lowest excitonic states decayed with a single-exponential time constant of 4.5 ± 0.2 ns. Furthermore, excitons in $CsPbBr_3$ QDs can be efficiently dissociated in the presence of electron or hole acceptors. The half-lives of electron transfer (ET) to benzoquinone and subsequent charge recombination are 65 ± 5 ps and 2.6 ± 0.4 ns, respectively. The half-lives for hole transfer (HT) to phenothiazine and the subsequent charge recombination are 49 ± 6 ps and 1.0 ± 0.2 ns, respectively. The lack of electron and hole traps and fast interfacial ET and HT rates are key properties that may enable the development of efficient lead halide perovskite QDs-based light-harvesting and -emitting devices.

Colloidal semiconductor quantum dots (QDs) have been the subject of intense research due to their many attractive properties,[1] including size-tunable band gap,[2] high photoluminescence (PL) quantum yields (QYs),[3] excellent photostability,[4] and versatile chemical processability.[5] They have found promising applications in biological imaging,[6] light-emitting diodes,[7] third-generation solar cells,[8] and low-threshold lasers.[9] Previous research efforts were mostly focused on metal chalcogenide QDs whose optical and electronic properties are well-established.[5] Recently, a new family of colloidal QDs based on lead halide perovskites, $MPbX_3$ (M = CH_3NH_3, Cs; X = Cl, Br, I), was reported,[10] partially motivated by the tremendous success of $CH_3NH_3PbI_3$ solar cells with certified power conversion efficiencies exceeding 20%.[11] Quantum-confined $MPbX_3$ nanowires and nanoplatelets were also reported.[12] As-synthesized $MPbX_3$ QDs were found to have tunable PL wavelengths covering the whole visible spectrum, narrow PL bandwidths, and high PL QYs (50−90%) without any further surface treatments, making them a promising alternative to prototypical CdSe QDs for light-harvesting and -emitting applications.[10a,b,13]

Herein, using ultrafast transient absorption (TA) spectroscopy, we report the first study of the dynamics of carrier trapping and recombination within $CsPbBr_3$ perovskite QDs and their interfacial charge transfer (CT) to electron and hole acceptors (Scheme 1), which are essential processes for their light-harvesting and -emitting applications. $CsPbBr_3$ was chosen for this study because of its visible bandgap and better chemical stability than $CH_3NH_3PbX_3$. We found that the high PL QYs (~79%) could be attributed to negligible electron- or hole-trapping processes in $CsPbBr_3$ QDs: ~94% of lowest excitonic states decayed with a single-exponential time constant of 4.5 ± 0.2 ns. In the presence of benzoquinone (BQ) as electron

Scheme 1. Schematic Energy Level Diagram of $CsPbBr_3$ Quantum Dot−Benzoquinone and Quantum Dot−Phenothiazine Complexes and Possible Charge Separation and Recombination Pathways[a]

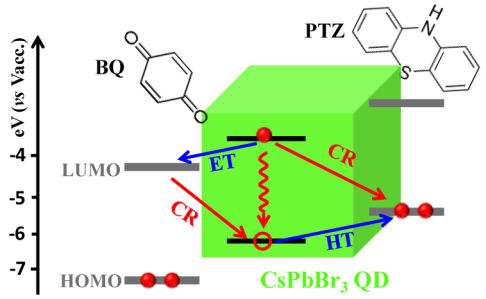

[a]The black solids lines indicate lowest energy electron and hole levels in quantum dots (QDs). The thick gray lines indicate lowest unoccupied molecular orbitals (LUMOs) and highest occupied molecular orbitals (HOMOs) of benzoquinone (BQ) and phenothiazine (PTZ) molecules. Forward charge separation processes, including electron transfer (ET) to BQ and hole transfer (HT) to PTZ, are shown by blue arrows, and backward charge recombination (CR) processes are shown by red arrows. Electron−hole recombination inside the QD is shown by a red wavy arrow.

Received: August 12, 2015
Published: September 28, 2015

DOI: 10.1021/jacs.5b08520
J. Am. Chem. Soc. 2015, 137, 12792−12795

acceptor, excitons in $CsPbBr_3$ QDs were efficiently dissociated by electron transfer (ET) with a half-life of 65 ± 5 ps, which was followed by charge recombination (CR) in the charge-separated state ($CsPbBr_3^+-BQ^-$) with a half-life of 2.6 ± 0.4 ns (eq 1). Hole transfer (HT) to phenothiazine (PTZ) occurred with a half-life of 49 ± 6 ps, and the charge-separated state $CsPbBr_3^--PTZ^+$ decayed with a half-life of 1.0 ± 0.2 ns (eq 2). The efficient ET and HT from perovskite QDs suggest their great potentials for use in light-harvesting and -emitting devices and may also provide important insights into the remarkable performance of bulk $MPbX_3$ perovskite film solar cells.[14]

$$CsPbBr_3{}^*-BQ \xrightarrow{ET} CsPbBr_3{}^+-BQ^- \xrightarrow{CR} CsPbBr_3-BQ \quad (1)$$

$$CsPbBr_3{}^*-PTZ \xrightarrow{HT} CsPbBr_3{}^-{}^+-PTZ^+ \xrightarrow{CR} CsPbBr_3-PTZ \quad (2)$$

$CsPbBr_3$ perovskite QDs were synthesized according to a recently reported hot injection procedure;[10b] details can be found in the Supporting Information (SI). These QDs typically exhibited orthorhombic shapes (Figure 1a) because they

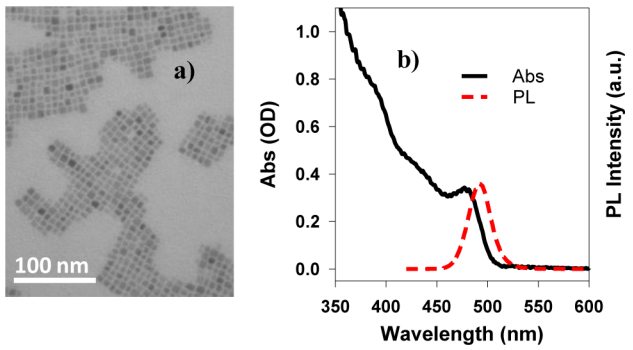

Figure 1. Transmission electron microscopy (TEM) image and absorption spectrum of $CsPbBr_3$ perovskite QDs. (a) Representative TEM image. (b) Absorption (black solid line) and photoluminescence (red dashed line) spectra of QDs dispersed in heptane.

crystallized in cubic perovskite phases, consistent with previous reports.[10b] Their average sizes, measured along long and short edges, were 7.4 ± 1.3 and 6.0 ± 1.0 nm (Figure S1), respectively. The short edge was considerably smaller than the estimated bulk Bohr exciton diameter (~7.4 nm).[10b] Quantum confinement leads to discrete electron and hole levels, and the optically allowed transitions between these levels give rise to discrete absorption bands in their UV–vis absorption spectrum (Figure 1b), with the lowest energy excitonic band (X1) centered at ~480 nm.[15] Based on this peak position and these bulk band edge positions,[16] we estimated the potentials of lowest electron and hole levels are at ~3.62 and 6.36 V versus vacuum, respectively. The PL peak was centered at 492 nm, with a full width at half-maximum of 130 meV. The PL QY of as-synthesized QDs was 79 ± 4% at 400 nm excitation, consistent with previously reported values,[10b] and much larger than those of as-synthesized CdSe core-only QDs (typically ~10–20%).[17]

Ultrafast TA spectroscopy studies were carried out to investigate the origin of exceptionally high PL QYs from these $CsPbBr_3$ QDs. The details of pump–probe TA set-ups are provided in the SI. Briefly, a pump pulse at 400 nm with tunable power density was used to excite the $CsPbBr_3$ QDs, and the induced absorption changes (ΔAbs), as functions of both wavelength and time, were recorded by a white light continuum probe pulse variably delayed with respect to the pump pulse. In all TA experiments discussed below, the power density was controlled to create ~0.025 exciton per QD (Figures S2–S4), and therefore the TA signals were dominated by QDs in the single exciton state. The TA spectra (Figure 2a)

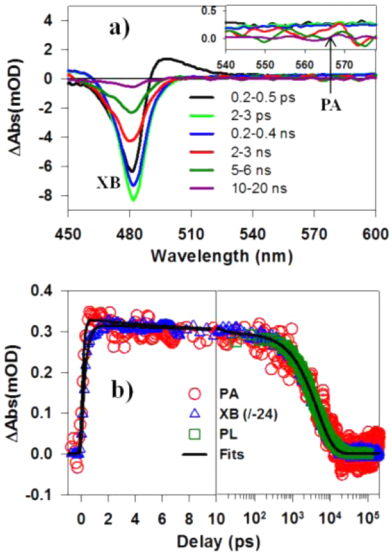

Figure 2. TA spectra and kinetics of $CsPbBr_3$ perovskite QDs measured with 400 nm excitation. (a) TA spectra of QDs at indicated delay time from 0.2 ps to 20 ns. Exciton bleach (XB) and photoinduced absorption (PA) features are labeled. (b) Kinetics of XB (blue triangles, reduced by a factor of 24 and inverted), PA (red circles), and PL decay (green squares) of QDs. The black solid lines are multi-exponential fits to these kinetics (see Table S1).

at early delay times (0.2–0.5 ps) showed an exciton bleach (XB) feature at ~480 nm and an exciton absorption (XA) feature at ~495 nm. Similar to CdSe QDs, XB and XA can be assigned to state-filling-induced bleach and hot-exciton-induced red-shift, respectively, of the X1 exciton band.[18] After hot-exciton relaxations (>2 ps), the exciton-induced shift was much smaller, and the TA spectra were dominated by the XB feature.

By selectively removing electrons from QDs using electron acceptors, we found that, in these $CsPbBr_3$ QDs, state fillings of the electron and hole levels contributed to ~67.2% and 32.8% of the XB feature, respectively (see Figures S6–S8 for details). This is different from CdX (X = S, Se, Te) QDs, where XB is dominated by electrons,[18] but similar to PbX QDs, where both electrons and holes contribute to XB.[19] According to previous calculations on bulk $CsPbBr_3$,[10b] the effective masses of electron and hole are similar, $0.15m_0$ (m_0 is the free electron mass) and $0.14m_0$, respectively. However, the valence band (VB) typically has higher degeneracy than the conduction band (CB), which might explain the higher contribution of electrons than holes to the XB feature. The TA spectra also showed a weak, broad photoinduced absorption (PA) feature throughout the visible region (with amplitude ~20 times weaker than XB), similar to PA signals observed in many other QDs.[20]

Kinetics of transient features are shown in Figure 2b. The XB feature (scaled and inverted for comparison) formed with a rise time of 0.32 ± 0.07 ps, corresponding to the hot carrier relaxation time into the lowest excitonic state (X1), and decayed with time constants (and amplitudes) of 8.4 ± 0.5 ps

DOI: 10.1021/jacs.5b08520
J. Am. Chem. Soc. 2015, 137, 12792–12795

(6.0 ± 0.5%) and 4.5 ± 0.2 ns (94.0 ± 0.7%). XB, PA, and PL decay kinetics agreed with each other (Table S1), although PL decay did not resolve <40 ps decay components due to its limited instrument response function. Because XB and PL depend on both electron and hole decay processes, the observed nearly single-exponential kinetics suggests minor contributions of independent electron- and/or hole-trapping pathways, and electron−hole pair radiative and nonradiative recombination is the dominant decay channel (~94%) in $CsPbBr_3$ QDs, which explains their high PL QY of ~79%.

BQ and PTZ molecules were used to measure the rates of ET and HT from photoexcited $CsPbBr_3$ QDs, respectively. The reduction and oxidation potentials for BQ and PTZ molecules are reported to be 4.3 V[21] and 5.5 V[20a] versus vacuum, corresponding to driving forces for ET and HT of 0.68 and 0.86 eV, respectively (Scheme 1). The TA spectra of $CsPbBr_3$ QD−BQ complexes at indicated delays from 2 ps to 20 ns after 400 nm excitation are shown in Figure 3a. Compared with free QDs, the XB decay in QD−BQ complexes was faster (Figure 3c), indicating ET from the CB of $CsPbBr_3$ QD to BQ. However, since both electrons and holes can contribute to the XB feature, the XB kinetics in QD−BQ complexes can also contain contributions from the subsequent CR process (Scheme 1). Faster XB decay in QD−PTZ complexes was also observed (Figure 3b,d), indicative of HT from the VB edge of $CsPbBr_3$ QD to PTZ. Similarly, the XB kinetics in QD−PTZ complexes can also contain contributions of the CR kinetics (Scheme 1). We also observed faster PA decay in both QD−BQ and QD−PTZ complexes than in free QDs, and PA kinetics always agreed with XB kinetics (Figure S9), indicating that the contributions of electron and hole in PA are similar to those in XB.

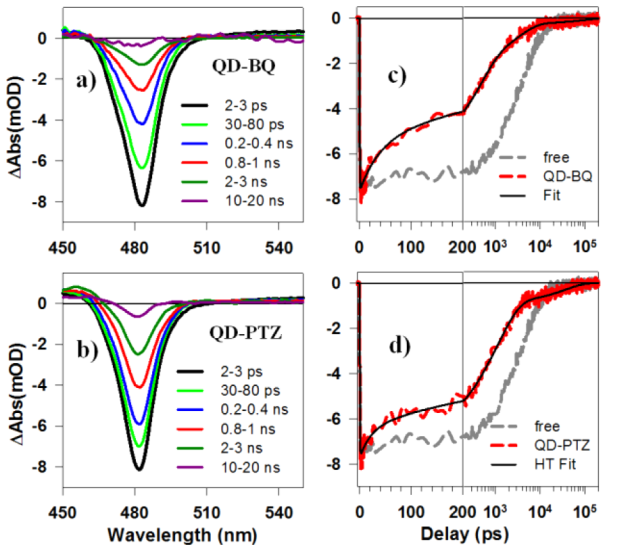

Figure 3. TA spectra and kinetics of QD−BQ and QD−PTZ complexes. TA spectra of (a) QD−BQ and (b) QD−PTZ complexes at indicated time delays after 400 nm excitation. Comparison of XB recovery kinetics in (c) QD−BQ and (d) QD−PTZ complexes (red dashed lines) with XB recovery kinetics in free QDs (gray dashed line). Black solid lines are multi-exponential fits to the kinetics according to the model described in the SI.

The XB kinetics in both QD−BQ and QD−PTZ complexes can be fitted with multi-exponential decays. According to the electron and hole contributions to the XB feature, the charge separation (CS) and CR amplitudes in QD−BQ are 67.2% and 32.8%, respectively, and the opposite in QD−PTZ. Details of the fitting model can be found in the SI. As shown in Figure 3c,d, this constrained model can successfully fit the XB kinetics in QD−BQ and QD−PTZ complexes. The fitting shows that, in QD−BQ complexes, ET and CR half-lives are 65 ± 5 ps and 2.6 ± 0.4 ns, respectively. In QD−PTZ complexes, HT and CR half-lives are 49 ± 6 ps and 1.0 ± 0.2 ns, respectively. Compared with the single-exciton half-lifetime of 2.8 ns in free QDs, the exciton dissociation efficiencies are near unity for both QD−BQ and QD−PTZ complexes.

We note that CT rates scale with number of acceptors on QD surfaces.[22] Because both BQ and PTZ are soluble in heptane, we measured acceptor concentration-dependent CT kinetics to estimate the average number of acceptors per QD, following a previously reported model.[23] The details of the experiments and model are provided in the SI (Figures S11 and S12, Tables S3 and S4), from which we estimate that the average number of BQ (PTZ) for the complexes studied in Figure 3 is 4.7 ± 0.7 (7.2 ± 1.5). Therefore, the fast CT rates and high CS efficiencies are enabled by the presence of multiple molecular acceptors. Nonetheless, in optoelectronic devices, materials such as TiO_2 and spiro-OMeTAD are used as electron and hole acceptors (or injection layers), respectively.[24] These materials typically have high densities of states and strong electronic couplings with QDs,[25] and therefore efficient ET and HT from perovskite QDs can be achieved. It is important to note that, in isolated QD−acceptor complexes studied here, efficient CS by either ET or HT is followed by fast CR due to the proximity of electron and hole. In perovskite film solar cells, electrons and holes are spatially separated because of the smaller exciton binding energy and have long carrier diffusion lengths.[26] Coupled with these properties, fast interfacial ET and HT at their respective extraction interfaces enable efficient long-distance CS, which may be responsible for their remarkable device efficiencies.[11]

In conclusion, we have investigated the ultrafast exciton dynamics and interfacial charge-transfer properties of $CsPbBr_3$ quantum dots. Using ultrafast transient absorption spectroscopy, we showed that the high photoluminescence quantum yields (~79%) of $CsPbBr_3$ QDs resulted from negligible electron- and hole-trapping pathways, and the decay of lowest excitonic states was dominated (94%) by a single-exponential channel with a time constant of 4.5 ns. Using benzoquinone and phenothiazine as electron and hole acceptors, respectively, excitons in $CsPbBr_3$ QDs were efficiently dissociated, with electron-transfer and hole-transfer half-lives of 65 ± 5 and 49 ± 6 ps, respectively. The half-lives of charge-separated states $CsPbBr_3^+$−BQ^- and $CsPbBr_3^-$−PTZ^+ were 2.6 ± 0.4 and 1.0 ± 0.2 ns, respectively. Our detailed spectroscopy assignments lay the foundation for understanding the photophysics of lead halide perovskite QDs-based light-harvesting and -emitting devices.[13] Furthermore, the observed efficient interfacial ET and HT from $CsPbBr_3$ QDs coupled with large carrier mobility may be key properties that are responsible for efficient perovskite film-based solar cells.

■ ASSOCIATED CONTENT

Supporting Information

The Supporting Information is available free of charge on the ACS Publications website at DOI: 10.1021/jacs.5b08520.

DOI: 10.1021/jacs.5b08520
J. Am. Chem. Soc. 2015, 137, 12792−12795

Sample synthesis, TA spectroscopy set-up, and kinetics fitting (PDF)

AUTHOR INFORMATION

Corresponding Author

*tlian@emory.edu

Author Contributions

#K.W. and G.L. contributed equally to this paper.

Notes

The authors declare no competing financial interest.

ACKNOWLEDGMENTS

The authors gratefully acknowledge the financial support from the National Science Foundation (CHE-1309817).

REFERENCES

(1) Alivisatos, A. P. *Science* **1996**, *271*, 933−937.

(2) Brus, L. E. *J. Chem. Phys.* **1984**, *80*, 4403−4409.

(3) (a) Hines, M. A.; Guyot-Sionnest, P. *J. Phys. Chem.* **1996**, *100*, 468−471. (b) Li, J. J.; Wang, Y. A.; Guo, W. Z.; Keay, J. C.; Mishima, T. D.; Johnson, M. B.; Peng, X. G. *J. Am. Chem. Soc.* **2003**, *125*, 12567−12575. (c) Chen, O.; Zhao, J.; Chauhan, V. P.; Cui, J.; Wong, C.; Harris, D. K.; Wei, H.; Han, H.-S.; Fukumura, D.; Jain, R. K.; Bawendi, M. G. *Nat. Mater.* **2013**, *12*, 445−451.

(4) Nirmal, M.; Brus, L. *Acc. Chem. Res.* **1999**, *32*, 407−414.

(5) Talapin, D. V.; Lee, J.-S.; Kovalenko, M. V.; Shevchenko, E. V. *Chem. Rev.* **2010**, *110*, 389−458.

(6) (a) Bruchez, M., Jr.; Moronne, M.; Gin, P.; Weiss, S.; Alivisatos, A. P. *Science* **1998**, *281*, 2013−2016. (b) Chan, W. C.; Nie, S. *Science* **1998**, *281*, 2016−2018.

(7) Shirasaki, Y.; Supran, G. J.; Bawendi, M. G.; Bulovic, V. *Nat. Photonics* **2013**, *7*, 13−23.

(8) (a) Nozik, A. J.; Beard, M. C.; Luther, J. M.; Law, M.; Ellingson, R. J.; Johnson, J. C. *Chem. Rev.* **2010**, *110*, 6873−6890. (b) Kramer, I. J.; Sargent, E. H. *Chem. Rev.* **2014**, *114*, 863−882.

(9) Klimov, V. I.; Mikhailovsky, A. A.; Xu, S.; Malko, A.; Hollingsworth, J. A.; Leatherdale, C. A.; Eisler, H. J.; Bawendi, M. G. *Science* **2000**, *290*, 314−317.

(10) (a) Zhang, F.; Zhong, H.; Chen, C.; Wu, X.-g.; Hu, X.; Huang, H.; Han, J.; Zou, B.; Dong, Y. *ACS Nano* **2015**, *9*, 4533−4542. (b) Protesescu, L.; Yakunin, S.; Bodnarchuk, M. I.; Krieg, F.; Caputo, R.; Hendon, C. H.; Yang, R. X.; Walsh, A.; Kovalenko, M. V. *Nano Lett.* **2015**, *15*, 3692−3696. (c) Nedelcu, G.; Protesescu, L.; Yakunin, S.; Bodnarchuk, M. I.; Grotevent, M. J.; Kovalenko, M. V. *Nano Lett.* **2015**, *15*, 5635−5640. (d) Akkerman, Q. A.; D'Innocenzo, V.; Accornero, S.; Scarpellini, A.; Petrozza, A.; Prato, M.; Manna, L. *J. Am. Chem. Soc.* **2015**, *137*, 10276−10281. (e) Huang, H.; Susha, A. S.; Kershaw, S. V.; Hung, T. F.; Rogach, A. L. *Adv. Sci.* **2015**, DOI: 10.1002/advs.201500194. (f) Schmidt, L. C.; Pertegás, A.; González-Carrero, S.; Malinkiewicz, O.; Agouram, S.; Mínguez Espallargas, G.; Bolink, H. J.; Galian, R. E.; Pérez-Prieto, J. *J. Am. Chem. Soc.* **2014**, *136*, 850−853.

(11) (a) Park, N.-G. *J. Phys. Chem. Lett.* **2013**, *4*, 2423−2429. (b) Green, M. A.; Emery, K.; Hishikawa, Y.; Warta, W.; Dunlop, E. D. *Prog. Photovoltaics* **2015**, *23*, 1−9.

(12) (a) Zhang, D.; Eaton, S. W.; Yu, Y.; Dou, L.; Yang, P. *J. Am. Chem. Soc.* **2015**, *137*, 9230−9233. (b) Tyagi, P.; Arveson, S. M.; Tisdale, W. A. *J. Phys. Chem. Lett.* **2015**, *6*, 1911−1916.

(13) Yakunin, S.; Protesescu, L.; Krieg, F.; Bodnarchuk, M. I.; Nedelcu, G.; Humer, M.; De Luca, G.; Fiebig, M.; Heiss, W.; Kovalenko, M. V. *Nat. Commun.* **2015**, *6*, 8056.

(14) (a) Ponseca, C. S.; Savenije, T. J.; Abdellah, M.; Zheng, K.; Yartsev, A.; Pascher, T.; Harlang, T.; Chabera, P.; Pullerits, T.; Stepanov, A.; Wolf, J.-P.; Sundström, V. *J. Am. Chem. Soc.* **2014**, *136*, 5189−5192. (b) Stranks, S. D.; Eperon, G. E.; Grancini, G.; Menelaou, C.; Alcocer, M. J. P.; Leijtens, T.; Herz, L. M.; Petrozza, A.; Snaith, H. J. *Science* **2013**, *342*, 341−344. (c) Kulbak, M.; Cahen, D.; Hodes, G. *J. Phys. Chem. Lett.* **2015**, *6*, 2452−2456.

(15) Efros, A. L.; Rosen, M. *Annu. Rev. Mater. Sci.* **2000**, *30*, 475−521.

(16) Butler, K. T.; Frost, J. M.; Walsh, A. *Mater. Horiz.* **2015**, *2*, 228−231.

(17) (a) Murray, C. B.; Norris, D. J.; Bawendi, M. G. *J. Am. Chem. Soc.* **1993**, *115*, 8706−8715. (b) Qu, L. H.; Peng, Z. A.; Peng, X. G. *Nano Lett.* **2001**, *1*, 333−337.

(18) Klimov, V. I. *J. Phys. Chem. B* **2000**, *104*, 6112−6123.

(19) Yang, Y.; Rodríguez-Córdoba, W. E.; Lian, T. *J. Am. Chem. Soc.* **2011**, *133*, 9246−9249.

(20) (a) Huang, J. E.; Huang, Z. Q.; Jin, S. Y.; Lian, T. Q. *J. Phys. Chem. C* **2008**, *112*, 19734−19738. (b) McArthur, E. A.; Morris-Cohen, A. J.; Knowles, K. E.; Weiss, E. A. *J. Phys. Chem. B* **2010**, *114*, 14514−14520. (c) Tyagi, P.; Kambhampati, P. *J. Chem. Phys.* **2011**, *134*, 094706−10. (d) Zhu, H.; Song, N.; Rodríguez-Córdoba, W.; Lian, T. *J. Am. Chem. Soc.* **2012**, *134*, 4250−4257. (e) Wu, K.; Song, N.; Liu, Z.; Zhu, H.; Rodríguez-Córdoba, W.; Lian, T. *J. Phys. Chem. A* **2013**, *117*, 7561−7570. (f) Wu, K.; Liu, Z.; Zhu, H.; Lian, T. *J. Phys. Chem. A* **2013**, *117*, 6362−6372.

(21) Zhao, X.; Kitagawa, T. *J. Raman Spectrosc.* **1998**, *29*, 773−780.

(22) (a) Boulesbaa, A.; Issac, A.; Stockwell, D.; Huang, Z.; Huang, J.; Guo, J.; Lian, T. *J. Am. Chem. Soc.* **2007**, *129*, 15132−15133. (b) Zhu, H.; Yang, Y.; Hyeon-Deuk, K.; Califano, M.; Song, N.; Wang, Y.; Zhang, W.; Prezhdo, O. V.; Lian, T. *Nano Lett.* **2014**, *14*, 1263−1269. (c) Song, N.; Zhu, H.; Jin, S.; Zhan, W.; Lian, T. *ACS Nano* **2011**, *5*, 613−621.

(23) (a) Morris-Cohen, A. J.; Frederick, M. T.; Cass, L. C.; Weiss, E. A. *J. Am. Chem. Soc.* **2011**, *133*, 10146−10154. (b) Wu, K.; Du, Y.; Tang, H.; Chen, Z.; Lian, T. *J. Am. Chem. Soc.* **2015**, *137*, 10224−10230.

(24) (a) Lee, M. M.; Teuscher, J.; Miyasaka, T.; Murakami, T. N.; Snaith, H. J. *Science* **2012**, *338*, 643−647. (b) Tan, Z.-K.; Moghaddam, R. S.; Lai, M. L.; Docampo, P.; Higler, R.; Deschler, F.; Price, M.; Sadhanala, A.; Pazos, L. M.; Credgington, D.; Hanusch, F.; Bein, T.; Snaith, H. J.; Friend, R. H. *Nat. Nanotechnol.* **2014**, *9*, 687−692.

(25) Yang, Y.; Rodríguez-Córdoba, W.; Xiang, X.; Lian, T. *Nano Lett.* **2012**, *12*, 303−309.

(26) (a) Shi, D.; Adinolfi, V.; Comin, R.; Yuan, M.; Alarousu, E.; Buin, A.; Chen, Y.; Hoogland, S.; Rothenberger, A.; Katsiev, K.; Losovyj, Y.; Zhang, X.; Dowben, P. A.; Mohammed, O. F.; Sargent, E. H.; Bakr, O. M. *Science* **2015**, *347*, 519−522. (b) Dong, Q.; Fang, Y.; Shao, Y.; Mulligan, P.; Qiu, J.; Cao, L.; Huang, J. *Science* **2015**, *347*, 967−970.

DOI: 10.1021/jacs.5b08520
J. Am. Chem. Soc. 2015, 137, 12792−12795